Langley Memorial Aeronautical Laboratory

1111-1
Copy No. 2 115
ACR No. 4B05

CLASSIFICATION CANCELLED

NATIONAL ADVISORY COMMITTEE FOR AERONAUTICS

UNCLASSIFIED

ADVANCE CONFIDENTIAL REPORT

A CONCISE THEORETICAL METHOD FOR PROFILE-DRAG CALCULATION

By Gerald E. Nitzberg

Ames Aeronautical Laboratory
Moffett Field, Calif.

UNCLASSIFIED

FOR REFERENCE
NOT TO BE TAKEN FROM THIS ROOM

CLASSIFIED DOCUMENT
This document contains classified information affecting the National Defense of the United States within the meaning of the Espionage Act, USC 50:31 and 32. Its transmission or the revelation of its contents in any manner to an unauthorized person is prohibited by law. Information so classified may be imparted only to persons in the military and naval Services of the United States, appropriate civilian officers and employees of the Federal Government who have a legitimate interest therein, and to United States citizens of known loyalty and discretion who of necessity must be informed thereof.

February 1944

CA019196

BEST

AVAILABLE

COPY

[redacted]

3 1176 01365 3358

NATIONAL ADVISORY COMMITTEE FOR AERONAUTICS

[redacted]

A CONCISE THEORETICAL METHOD FOR PROFILE-DRAG CALCULATION

By Gerald E. Nitzberg

SUMMARY

In this report a method is presented for the calculation of the profile drag of airfoil sections. The method requires only a knowledge of the theoretical velocity distribution and can be applied readily once this distribution is ascertained. Comparison of calculated and experimental drag characteristics for several airfoils shows a satisfactory agreement. Sample calculations are included.

INTRODUCTION

H. B. Squire and A. D. Young developed a method, presented in reference 1, for calculating the profile drag over an arbitrary airfoil. This method requires a knowledge of the velocity distribution over the airfoil, and of the estimated position of transition from laminar to turbulent flow. The velocity distribution can be obtained by the method of reference 2. Using these data the growth of the boundary layer can be computed, the region of the laminar flow being analyzed by means of a step-by-step solution of Pohlhausen's equation, and the turbulent region by a similar method of solution of an equation developed in reference 1. From the thickness of the boundary layer and the local velocity at the airfoil trailing edge, Squire and Young evaluate the profile drag by means of a semi-empirical formula. This procedure is very laborious because of the step-by-step computations involved, and its application is limited by lack of a method for estimating the position of transition.

E. N. Jacobs and A. E. von Doenhoff (reference 3) give formulas for estimating the transition position for velocity distributions having maximum velocity far

back, and T. von Karman and C. Millikan (reference 4) indicate a means for obtaining this information for velocity distributions with maximum velocity far forward. In these references methods are presented for directly calculating the boundary-layer growth in the laminar region. These methods, taken in conjunction with the concise graphical method for analyzing the region of turbulent flow, which is developed in the present report, make it possible to calculate quickly the profile-drag coefficient of an arbitrary airfoil. This procedure is outlined in a readily usable form. Several illustrative examples are worked in detail and the calculated results are compared with experimental measurements.

THEORY

The profile drag of an airfoil in free air is accounted for by the momentum loss in the wake far downstream. It is possible to calculate this momentum loss by tracing the boundary-layer growth along the airfoil surface and its development, as the wake, after leaving the airfoil trailing edge. The growth of the boundary layer is a function of the chordwise velocity distribution over the airfoil. In studying this growth the essential factors are:

1. Position of transition from laminar to turbulent flow

2. Boundary-layer thickness at transition

3. Growth of the turbulent boundary layer

Once the thickness of the boundary layer at the trailing edge has been computed the pressure recovery in the wake can be accounted for by the semi-empirical theory of Squire and Young. These various steps will now be considered in detail.

1. Transition point.- The profile drag of airfoils is markedly affected by the position of transition from laminar to turbulent flow. For smooth airfoils in low turbulence streams at Reynolds numbers of the order of 5,000,000, transition generally occurs close to the

laminar separation point. Surface roughness, stream turbulence, or an extremely high Reynolds number can move transition forward of this point. For airfoils having maximum velocity far forward, however, there is no practical method available for predicting the extent of this movement of transition ahead of the separation point. In such cases therefore, transition position will be assumed to coincide with separation. It is convenient to make this simplification because reference 4 contains a direct method for calculating the separation point of airfoils having maximum velocity far forward. This method approximates the forward portion of the chordwise velocity distribution by two straight lines. The region ahead of maximum velocity is represented by

$$\frac{V}{V_0} = a\left(\frac{x}{c}\right) \qquad (1)$$

and the region directly behind maximum velocity by

$$\frac{V}{V_0} = (a + b)\frac{x_m}{c} - b\left(\frac{x}{c}\right) \qquad (2)$$

where the subscript m designates the coordinate of the maximum velocity point. It can be shown from reference 4 that the velocity at separation V_s is a function of the slopes of the approximating straight lines and the maximum velocity V_m; namely,

$$\frac{V_m}{V_s} = \Phi_s \qquad (3)$$

where Φ_s is the function of b/a plotted in figure 1.

For low-drag airfoils which have maximum velocity far back, separation occurs so closely behind maximum velocity that transition may be assumed to lie at that position, except at very high Reynolds numbers where it is possible for transition to move ahead of the maximum velocity point. As is pointed out in reference 3, existing experimental data taken in flight indicate that transition will occur in a region of increasing velocity if the boundary-layer Reynolds number reaches a value of the order of 8000 to 9500. It is possible to apply this criterion by using the relation given in reference 3

for calculating the boundary-layer Reynolds number in a region of increasing velocity,

$$\frac{R_\delta^2}{R} = 5.3 \left(\frac{V_0}{V_1}\right)^{7.17} \int_0^{x/c} \left(\frac{V}{V_0}\right)^{3.17} d\left(\frac{x}{c}\right) \qquad (4)$$

where

$R_\delta = \frac{\delta V_1}{\nu}$ boundary-layer Reynolds number

$R = \frac{V_0 c}{\nu}$ airfoil Reynolds number

δ distance normal to the surface from the surface to the point in the boundary layer at which the velocity is $0.707V_1$

V_1 velocity outside boundary layer at the point for which boundary layer is being computed

V_0 free-stream velocity

V velocity outside the boundary layer at any value of x/c

x distance along airfoil surface from leading edge

c airfoil chord

By the use of equation (3) or (4) it is possible to find the approximate location of the transition point for most airfoil velocity distributions.

2. Boundary-layer thickness at transition.- The growth of the turbulent boundary layer depends upon the initial boundary-layer thickness after transition. Flight experiments indicate that transition occurs abruptly at a point. Since there is no appreciable drag over such a small region, the momentum thickness of the boundary layer, θ, remains unchanged in passing from laminar to turbulent flow. Moreover, for a Blasius velocity profile the momentum thickness is related to the boundary-layer thickness by

$$\theta = 0.289\ \delta \qquad (5)$$

Therefore if the thickness of the laminar boundary layer at transition is computed, the initial value of the turbulent momentum thickness is also known.

Squire and Young studied the momentum thickness in terms of the factor ζ. The relation, given in reference 1, between these quantities is

$$\zeta = 2.56 \log_e \left[4.075 \frac{V\theta}{\nu} \right] \tag{6}$$

The laminar boundary-layer thickness at transition can be calculated by the methods of references 3 and 4. From reference 4 it can be shown that when the velocity distribution can be approximated by the straight lines of equations (1) and (2), then

$$\frac{V\delta}{\nu} = \frac{\Delta_s}{1.79} \left(\frac{x_m}{c} \right) \sqrt{\frac{a}{2}} \sqrt{R} \tag{7}$$

where Δ_s, the function of the ratio of the slopes of the straight lines, b/a, is plotted in figure 1. Substituting equations (5) and (7) into equation (6) gives as the approximate initial value of the ζ factor when the position of maximum velocity is far forward

$$\zeta_1 = 2.56 \log_e \left[0.66 \, \Delta_s \left(\frac{x_m}{c} \right) \sqrt{\frac{a}{2}} \sqrt{R} \right] \tag{8}$$

In reference 3 the relation given for the laminar boundary-layer thickness in a region of increasing velocity is

$$\left(\frac{\delta}{c} \right)^2 = \frac{5.3}{R} \left(\frac{V_o}{V_1} \right)^{9.17} \int_{o}^{x/c} \left(\frac{V}{V_o} \right)^{8.17} d\left(\frac{x}{c} \right) \tag{9}$$

Therefore, for this case of transition occurring in a region of increasing velocity, equation (6) takes the form

$$\zeta_i = 2.56 \log_e \left[1.18 \left(\frac{\delta_i}{c} \right) \left(\frac{V_i}{V_o} \right) R \right] \tag{10}$$

Equation (8) for the "double-roof" velocity distributions and equation (10) for "low-drag" velocity distributions are adequate for finding the initial value of the ζ factor for most airfoils.

3. Turbulent boundary-layer growth.- The analysis of the turbulent boundary layer is based on equation (11) (p. 8 of reference 1).

$$\frac{d\zeta}{d\left(\frac{x}{c}\right)} = \frac{10.41\,R}{\zeta^2}\left(\frac{V}{V_o}\right)e^{-0.3914\zeta} - 6.13\,\frac{V'}{V} \qquad (11)$$

where

$\zeta = \left(\frac{\rho V^2}{\tau_o}\right)^{\frac{1}{2}}$ the ζ factor

τ_o intensity of skin friction

Prime indicates derivative with respect to (x/c)

Squire and Young use a step-by-step integration to solve this equation. This process is very laborious and can be simplified to a direct graphical evaluation without loss of accuracy. The simplification is as follows:

Divide the velocity distribution in the turbulent region at those positions where its slope changes rapidly. Approximate each of these segments by a curve of the form

$$\frac{x}{c} = \frac{K}{(V/V_o)} + L \qquad (12)$$

where K and L are constants determined by making curve 12 pass through the end points of the velocity-distribution segment under consideration. For a region of decreasing velocity, substituting equation (12) in equation (11) leads to

$$\frac{d\zeta}{KFR + 6.13} = -\frac{d\left(\frac{V}{V_o}\right)}{\frac{V}{V_o}}$$

or $$\int_{\zeta_1}^{\zeta_2} \frac{d\zeta}{KFR+6.13} = \log_e \frac{V_1}{V_2} \qquad (13)$$

where

$$F = 10.41\ \zeta^{-2}\ e^{-0.3914\zeta}$$

It is also possible to separate the variables of equation (11) by replacing the actual velocity distribution in each segment by its average velocity and average gradient. This alternative method leads to an integral of form similar to the left-hand side of equation (13) and gives the same value for the ζ factor. There is, therefore, no need for further considering this alternative procedure.

The left side of equation (13) cannot be integrated by elementary means. By numerical integration

$$\int_0^{\zeta} \frac{d\zeta}{KFR+6.13}$$

has been evaluated for the usual range of ζ and KR. These values are given in table I and plotted in figure 2. Therefore, when ζ_1, K, R, and $\log_e \left(\frac{V_1}{V_2}\right)$ are known, the value of ζ_2 may be found from figure 2 by using equation (13) in the form

$$I = \int_0^{\zeta_2} \frac{d\zeta}{KFR+6.13} = \log_e \left(\frac{V_1}{V_2}\right) + \int_0^{\zeta_1} \frac{d\zeta}{KFR+6.13} \qquad (14)$$

Equation (14) applies only in regions over which the velocity decreases. When the velocity remains constant, equation (11) simplifies to

$$R\left(\frac{V}{V_o}\right)\left(\frac{x_2 - x_1}{c}\right) = \frac{1}{10.41}\int_{\zeta_1}^{\zeta_2} \zeta^2 \, e^{0.3914\zeta} \, d\zeta \qquad (15)$$

$$= e^{0.3914\zeta_2}\left[0.2454\zeta_2^2 - 1.254\zeta_2 + 3.204\right]$$

$$- e^{0.3914\zeta_1}\left[0.245\zeta_1^2 - 1.254\zeta_1 + 3.204\right]$$

which can be solved by the use of figure 3.

In a region over which the velocity is increasing, equation (14) is replaced by

$$\int_{\zeta_o}^{\zeta_2} \frac{d\zeta}{KFR - 6.13} = \log_e\left(\frac{V_2}{V_1}\right) + \int_{\zeta_o}^{\zeta_1} \frac{d\zeta}{KFR - 6.13} \qquad (16)$$

values for the integral appearing in equation (16) have been evaluated and are given in table II and figure 4.

It is rarely necessary to divide the velocity distribution in the region of turbulent flow into any more than three segments. In each of these segments either equation (14), (15), or (16) will apply. Therefore the increase of ζ through the turbulent region can be calculated directly by the use of figures 2, 3, and 4.

Calculation of the drag coefficient.- Squire and Young have shown in reference 1 that when the final value of the momentum thickness, θ_T, and the relative velocity at the trailing edge of an airfoil are known the drag coefficient can be calculated by the relation

$$C_D = 2\left(\frac{\theta_T}{c}\right)\left(\frac{V_T}{V_o}\right)^{3.2} \qquad (17)$$

where the subscript T indicates values at the trailing edge. The previous analysis has been in terms of the ζ factor; so, to avoid having to convert to terms of momentum thickness, it is possible to use equation (6) rewritten as

$$\frac{V\theta}{v} = 0.2454\, e^{0.3914\zeta} = \lambda \qquad (18)$$

Substituting into equation (17) gives as the profile-drag coefficient

$$C_D = \frac{2\lambda_T}{R}\left(\frac{V_T}{V_o}\right)^{2.2} \qquad (19)$$

In figure 5, λ is plotted as a function of ζ. Therefore, when the value of ζ_T has been computed, λ_T can be read from figure 5, and the profile drag can then be calculated by equation (19).

APPLICATION

The method for calculating the profile drag, which is outlined in the previous section, can best be illustrated by indicating the actual steps in the calculation of several examples.

Example 1. Low-drag airfoil at high lift.- The velocity distribution for the NACA 35-215 airfoil was computed at a lift coefficient of 1.22 by the method of reference 2 and is given by the solid line in figure 6. The trailing-edge velocity was obtained by extrapolating the calculated velocity gradient near the trailing edge. Distances along the airfoil surface are nearly the same as distances along the chord except at the leading edge. Since at the leading edge the method of reference 4 for laminar boundary layers applies, and this method is not significantly affected by replacing distances along the surface by their chordwise component, it is possible to make the simplification of using chordwise distances instead of actual lengths along the airfoil surface. This simplification is usually permissible.

The computed velocity distribution has stagnation point at $x/c = 0.0270$ on the lower surface and a maximum velocity of 2.392 times free stream at $x/c = 0.0037$ on the upper surface. Behind this point the velocity reaches $V/V_o = 2.210$ at $x/c = 0.0108$. Therefore, from equation (1)

$$a = \frac{2.392}{0.0270 + 0.0037} = 78.0$$

and equation (2)

$$b = \frac{2.392 - 2.210}{0.0108 - 0.0037} = 25.6$$

from figure 1, since $b/a = 0.33$,

$$\Phi_s = 1.054, \qquad \Delta_s = 6.0$$

equation (3) gives as the velocity at transition (separation)

$$V_s = \frac{2.392}{1.054} = 2.27$$

which corresponds to a value of $x/c = 0.0090$. If the Reynolds number is taken to be 5.75×10^6, the ζ factor at transition by equation (8) is

$$\zeta_i = 2.56 \log_e \left[0.66\ (6)\ (0.0307)\ \sqrt{39}\ \sqrt{5.75}\ \ 10^3 \right] = 19.2$$

The positions in the turbulent region of the upper surface at which the velocity gradient changes abruptly are approximately: $x/c = 0.0727$, $V/V_0 = 1.725$ and $x/c = 0.50$, $V/V_0 = 1.432$. Using $V/V_0 = 0.768$ as the trailing-edge velocity, it is now possible to trace the growth of ζ. By equation (12)

$$K_1 R = \frac{(0.0727 - 0.0090)}{\left(\frac{1}{1.725}\right) - \left(\frac{1}{2.27}\right)}\ 5.75 \times 10^6 = 2.62 \times 10^6$$

and then from equation (14) and figure 2

$$I_1 = 0.042 + \log_e \left(\frac{2.27}{1.725}\right) = 0.316$$

so that from figure 2

$$\zeta_{x/c = 0.073} = 24.05$$

Similarly

$$K_2R = \frac{(0.500 - 0.073)}{\left(\frac{1}{1.432}\right) - \left(\frac{1}{1.725}\right)} 5.75 \times 10^6 = 20.8 \times 10^6$$

$$I_2 = 0.060 + \log_e \left(\frac{1.725}{1.432}\right) = 0.247$$

$$\zeta_{x/c = 0.50} = 27.60$$

$$K\,R = \frac{(1.00 - 0.50)}{\left(\frac{1}{0.768}\right) - \left(\frac{1}{1.432}\right)} 5.75 \times 10^6 = 4.77 \times 10^6$$

$$I_3 = 0.592 + \log_e \left(\frac{1.432}{0.768}\right) = 1.216$$

$$\zeta_T = 31.90$$

From figure 5

$$\lambda_T = 6.50 \times 10^4$$

The lower surface has a maximum velocity of $V/V_0 = 0.963$ at $x/c = 0.55$. Assuming that transition occurs at the point of maximum velocity, the initial ζ factor is found from equation (9)

$$\left(\frac{\delta}{c}\right)^2 = \frac{5.3}{5.75 \times 10^6} \left(\frac{1}{0.963}\right)^{9.17} (0.158) = 0.206 \times 10^{-6}$$

and equation (10)

$$\zeta_i = 2.56 \log_e \left[1.18 \sqrt{0.206 \times 10^6}\ (0.963) 5.75 \times 10^6\right] = 20.5$$

The final ζ factor is found by equations (12), (14), and figure 2.

$$KR = \frac{(1.00 - 0.50)}{\left(\frac{1}{0.768}\right) - \left(\frac{1}{0.963}\right)} 5.75 \times 10^6 = 10.88 \times 10^6$$

$$I = 0.022 + \log\left(\frac{0.963}{0.768}\right) = 0.248$$

and

$$\zeta_T = 26.2$$

from figure 5

$$\lambda_T = 0.69 \times 10^4$$

Finally, substituting the value of λ_T of the upper plus the lower surface in equation (19) gives

$$C_D = \frac{2(6.50 + 0.69) \times 10^4}{5.75 \times 10^6} (0.768)^{2.2} = 0.0140$$

Example 2. Transition ahead of maximum velocity.- As another illustration of the methods for calculating the profile drag, the drag of the experimental velocity distribution for the NACA 66,2-420 airfoil at zero angle of attack, given in reference 5, will be calculated for transition fixed at $x/c = 0.10$ on both surfaces at a Reynolds number of 6.35×10^6, corresponding to a Mach number of 0.194. The upper and lower surfaces are treated as being divided into two turbulent regions each. These divisions are shown on the plot of the experimental velocity distribution (fig. 7). The analysis is based on equation (9), (10), (12), and (16). For the upper surface:

$$\left(\frac{\delta}{c}\right)^2 = \frac{5.3\ (0.252)}{6.35\ (5.3)} 10^{-6} = 0.0395 \times 10^{-6}$$

$$\zeta_i = 2.56 \log_e \left[1.18\ (0.199 \times 10^{-3})\ 1.2\ (6.35)\ 10^6\right] = 19.2$$

$$KR = \frac{(0.60 - 0.10)}{\left(\frac{1}{1.20}\right) - \left(\frac{1}{1.32}\right)} 6.35 \times 10^6 = 41.2 \times 10^6$$

$$I_1 = 0.001 + \log\left(\frac{1.32}{1.20}\right) = 0.095$$

from figure 4

$$\zeta_{o\ 60} = 26.0$$

$$K_2R = \frac{(1.00 - 0.60)}{\left(\frac{1}{0.86}\right) - \left(\frac{1}{1.32}\right)}\ 6.35 \times 10^6 = 6.28 \times 10^6$$

$$I_2 = 0.333 + \log\left(\frac{1.32}{0.86}\right) = 0.761$$

from figure 2

$$\zeta_T = 29.4$$

and figure 5 gives

$$\lambda_T = 2.42 \times 10^4$$

For the lower surface:

$$\left(\frac{\delta}{c}\right)^* = \frac{5.3\ (0.161)}{6.35\ (2.71)}\ 10^{-6} = 0.050 \times 10^{-6}$$

$$\zeta_i = 2.56 \log_e \left[1.18\ (0.223 \times 10^{-3})\ 1.12\ (6.35)\ 10^6\right] = 19.3$$

$$K_1R = \frac{(0.60 - 0.10)}{\left(\frac{1}{1.12}\right) - \left(\frac{1}{1.18}\right)}\ 6.35 \times 10^6 = 72.2 \times 10^6$$

$$I_1 = 0.00 + \log\left(\frac{1.18}{1.12}\right) = 0.053,\quad \zeta_{o,60} = 26.0$$

$$K_2R = \frac{(1.00 - 0.60)}{\left(\frac{1}{0.86}\right) - \left(\frac{1}{1.18}\right)}\ 6.35 \times 10^6 = 8.06 \times 10^6$$

$$I_2 = 0.286 + \log\left(\frac{1.18}{0.86}\right) = 0.602,\quad \zeta_T = 28.8$$

and from figure 5

$$\lambda_T = 1.92 \times 10^4$$

The drag coefficient is therefore

$$C_D = \frac{2\,(2.42+1.92)\times 10^4}{6.35\times 10^6}\,(0.86)^{2.2} = 0.0098$$

The profile drag of most airfoils can be calculated by the use of the operations involved in these two examples.

DISCUSSION AND CONCLUSIONS

The graphical method for analyzing the turbulent region, presented and illustrated in the previous sections, uses a rough approximation to the velocity distribution. It is possible to use such an approximation because the growth of the turbulent boundary layer seems rather insensitive to the actual shape of the velocity distribution in a region over which the velocity gradient does not change markedly. This point can be illustrated by considering the upper surface velocity distribution of the NACA 35-215 airfoil in figure 6. It is seen that the turbulent region has three markedly different regions. When the calculation is based on these natural divisions, the value found for the profile-drag coefficient is 0.0140 (example 1). Further division of the velocity distribution fails to change this value. On the other hand, if the natural divisions are not taken into account, the calculated drag coefficient is considerably in error. For example, if the above turbulent region is treated as a single segment, the drag coefficient is 0.0126, and when treated as two segments the drag coefficient is 0.0159.

The theoretical velocity distributions obtained by the method of reference 2 have the shortcoming of having a stagnation point at the trailing edge. In order to compensate for this incorrect trailing-edge velocity, it is necessary to extrapolate the velocity gradient from ahead of about $x/c = 0.9$. The error involved in such

an approximation is rather small because changes in the skin friction, due to trailing-edge velocity variations, are compensated for by the corresponding changes in the pressure drag. This can be illustrated by assuming for the trailing-edge velocity in figure 6 a value of $V/V_0 = 0.90$. The calculated profile-drag coefficient for this new trailing-edge velocity is 0.0136, which is in satisfactory agreement with the previously calculated value of 0.0140.

The experimentally measured velocity distributions and profile-drag coefficients for a wide range of lift coefficients of the NACA 35-215 airfoil are presented in reference 6. Theodorsen's method, reference 2, also was used to calculate the theoretical velocity distributions for the NACA 35-215 airfoil at a number of lift coefficients. The calculations were made at specific lift coefficients rather than specific angles of attack because the distributions thus obtained more nearly approximate experimental measurements. The profile-drag coefficients at these lifts were calculated from both the theoretical and the experimental velocity distributions. The values thus obtained are compared with the experimentally measured polar in figure 8. The position of transition for the low-drag range of lift coefficients was found experimentally to lie from 5 to 10 percent of the chord length behind the position of maximum velocity. The calculated low-drag coefficients assume transition to occur at the position of maximum velocity and consequently these computed values are higher than the experimental values.

The profile-drag coefficients and experimental pressure distributions over a wide range of Mach numbers, and corresponding Reynolds numbers, are given in reference 5 for an NACA 66,2-420 airfoil. The procedure of the present report has been used to calculate the drag at various Mach numbers for the smooth airfoil with transition fixed at $x/c = 0.10$, both at 0° angle of attack. These calculated values are compared with the experimentally measured profile drags in figure 9. The values for the smooth airfoil are in good agreement with experimental measurements up to about $M = 0.53$, which corresponds to a Reynolds number of 16×10^6. Above this Mach number the measured drag increases rapidly because transition moves ahead of the position of maximum velocity. Since the turbulence level of the tunnel is higher than that of free air, the boundary-layer Reynolds number at transition is well below the value of 8000 which

was mentioned as a criterion for transition on a smooth airfoil in flight. Moreover, as is shown in reference 7, compressibility effects produce a profound change in boundary-layer Reynolds number at transition. So, lacking knowledge of the proper transition criterion to use for the wind tunnel in which these tests were made, transition on the smooth airfoil was assumed to occur at the maximum velocity position. The calculated values for the case of transition fixed at $x/c = 0.10$ are uniformly lower than the experimental points because the theory does not account for the drag of the carborundum used to fix transition. When transition was fixed at $x/c = 0.60$, the experimentally measured drag coefficient was about 0.0009 above the measured values for the smooth airfoil. This drag increase is due chiefly to the carborundum strip. Since transition at $x/c = 0.10$ was fixed by a similar carborundum strip, it is to be expected that the drag of the carborundum in this case also will be about 0.0009. When this amount is added to the theoretically calculated drag, the calculated values are in satisfactory agreement with the experimental measurements.

As a further comparison of the results predicted, by the methods presented here, with experimental measurements, polars for the NACA 67,1-215 airfoil have been calculated for Reynolds numbers of 2.9×10^6 and 6.0×10^6. The experimentally measured polars at these Reynolds numbers and a simple method for computing the velocity over low-drag airfoils at various lift coefficients are presented in reference 8. In figure 10 the experimental measurements are compared with the theoretically calculated polars. The large discrepancies in the drag coefficients for high lift coefficients may be due to "turbulent separation" on the upper surface of the airfoil. Such a breakdown of the flow is believed to occur when a thick turbulent boundary layer is subjected to a steep adverse pressure gradient. To determine the limits of applicability of the present method, polars were calculated for a number of widely different airfoils. Satisfactory agreement with experimental measurements was found up to lift coefficients for which the drag coefficient of the surface of highest drag on the airfoil was somewhat greater than 0.01. With higher lift coefficients the calculated drag coefficients were progressively lower than the measured values. It is also seen from figure 10 that an incorrect variation of the lift coefficients with

Reynolds number corresponding to the end points of the low-drag region is predicted by the present method. This shortcoming results from the lack of an adequate criterion for determining the transition-point movement caused by the velocity peak at the forward part of the airfoil. This peak arises from the superposition of small additional and basic low-drag velocity distributions.

The problem of sudden shifts in transition point with small changes in lift coefficient is not limited to low-drag airfoils. In figure 11 the calculated polar of the NACA 23015 airfoil is compared with the experimental measurements given in reference 8. It is seen that the abrupt drag increase in the wind tunnel at small negative lift coefficients occurs at a different lift coefficient from that predicted. Moreover, figure 11 indicates that the drag coefficients for conventional as well as low-drag airfoils can be calculated for wide ranges of lift coefficients.

Ames Aeronautical Laboratory,
National Advisory Committee for Aeronautics,
Moffett Field, Calif.

REFERENCES

1. Squire, H. B., and Young, A. D.: The Calculation of of the Profile Drag of Aerofoils. R. & M. No. 1838, British A.R.C., 1938.

2. Theodorsen, Theodore: Theory of Wing Sections of Arbitrary Shape. NACA Rep. No. 411, 1931.

3. Jacobs, E. N., and von Doenhoff, A. E.: Formulas for Use in Boundary-Layer Calculations on Low-Drag Wings. NACA ACR, Aug. 1941.

4. von Kármán, Th., and Millikan, C. B.: On the Theory of Laminar Boundary Layers Involving Separation. NACA Rep. No. 504, 1934.

5. Hood, Manley J., and Anderson, Joseph L.: Tests of an NACA 66,2-420 Airfoil of 5-Foot Chord at High Speed. NACA ACR., Sept. 1942.

6. Allen, H. Julian, and Frick, Charles W., Jr.: Experimental Investigation of a New Type of Low-Drag Wing-Nacelle Combination. NACA ACR, July 1942.

7. Allen, H. Julian, and Nitzberg, Gerald E.: The Effect of Compressibility on the Growth of the Laminar Layer on Low-Drag Wings and Bodies. NACA ACR, Jan. 1943.

8. Jacobs, Eastman N., Abbott, Ira H., and Davidson, Milton: Preliminary Low-Drag-Airfoil and Flap Data From Tests at Large Reynolds Numbers and Low Turbulence. NACA ACR and Supplement, March 1942.

TABLE I.– VALUES OF $\int_{\zeta_0}^{\zeta} \frac{d\zeta}{KRF+6.13}$ FOR CALCULATING ζ IN

A REGION OF DECREASING VELOCITY

ζ \ KR	10^6	2×10^6	5×10^6	10^7	2×10^7	5×10^7	10^8
18.5	0.0787	0.0417	0.0177	0.0088	0.0044	0.0019	0.0009
19.5	.1220	.0666	.0287	.0145	.0073	.0030	.0015
20.5	.1827	.1039	.0459	.0237	.0120	.0049	.0025
21.5	.2628	.1571	.0723	.0380	.0195	.0080	.0040
22.5	.3623	.2300	.1112	.0601	.0314	.0130	.0066
23.5	.4793	.3210	.1661	.0931	.0497	.0209	.0106
24.5	.6104	.4305	.2396	.1403	.0774	.0332	.0170
25.5	.7518	.5555	.3321	.2048	.1176	.0520	.0270
26.5	.9006	.6925	.4420	.2881	.1738	.0798	.0425
27.5	1.0544	.8383	.5676	.3901	.2479	.1208	.0659
28.5	1.2116	.9900	.7050	.5086	.3409	.1774	.1001
29.5	1.3708	1.1458	.8508	.6406	.4520	.2520	.1485
30.5	1.5313	1.3041	1.0023	.7824	.5776	.3454	.2139
31.5	1.6930	1.4640	1.1581	.9314	.7147	.4560	.2975
32.5	1.8551	1.6251	1.3166	1.0852	.8503	.5813	.3993
33.5	2.0175	1.7867	1.4766	1.2421	1.0118	.7183	.5173

TABLE II.– VALUES OF $\int_{\zeta_0}^{\zeta} \frac{d\zeta}{KRF-6.13}$ FOR CALCULATING ζ

IN A REGION OF INCREASING VELOCITY

ζ \ KR	10^6	2×10^6	5×10^6	10^7	2×10^7	5×10^7	10^8
14.5	0.0113	0.0047	0.0020	0.0011	0.0003	0.0001	——
15.5	.0194	.0087	.0036	.0019	.0007	.0003	——
16.5	.0336	.0154	.0062	.0032	.0014	.0006	.0001
17.5	.0586	.0270	.0107	.0054	.0025	.0011	.0003
18.5	.1044	.0449	.0182	.0091	.0043	.0018	.0006
19.5	.1968	.0809	.0309	.0152	.0073	.0030	.0012
20.5	.4345	.1494	.0528	.0255	.0123	.0050	.0022
21.5	——	.3009	.0917	.0429	.0206	.0082	.0038
22.5	——	.8890	.1663	.0732	.0345	.0135	.0064
23.5	——	——	.3340	.1287	.0582	.0222	.0107
24.5	——	——	——	.2410	.1001	.0367	.0178
25.5	——	——	——	.5510	.1795	.0612	.0292
26.5	——	——	——	——	.3580	.1045	.0483
27.5	——	——	——	——	——	.1866	.0810
28.5	——	——	——	——	——	.3720	.1421
29.5	——	——	——	——	——	——	.2610

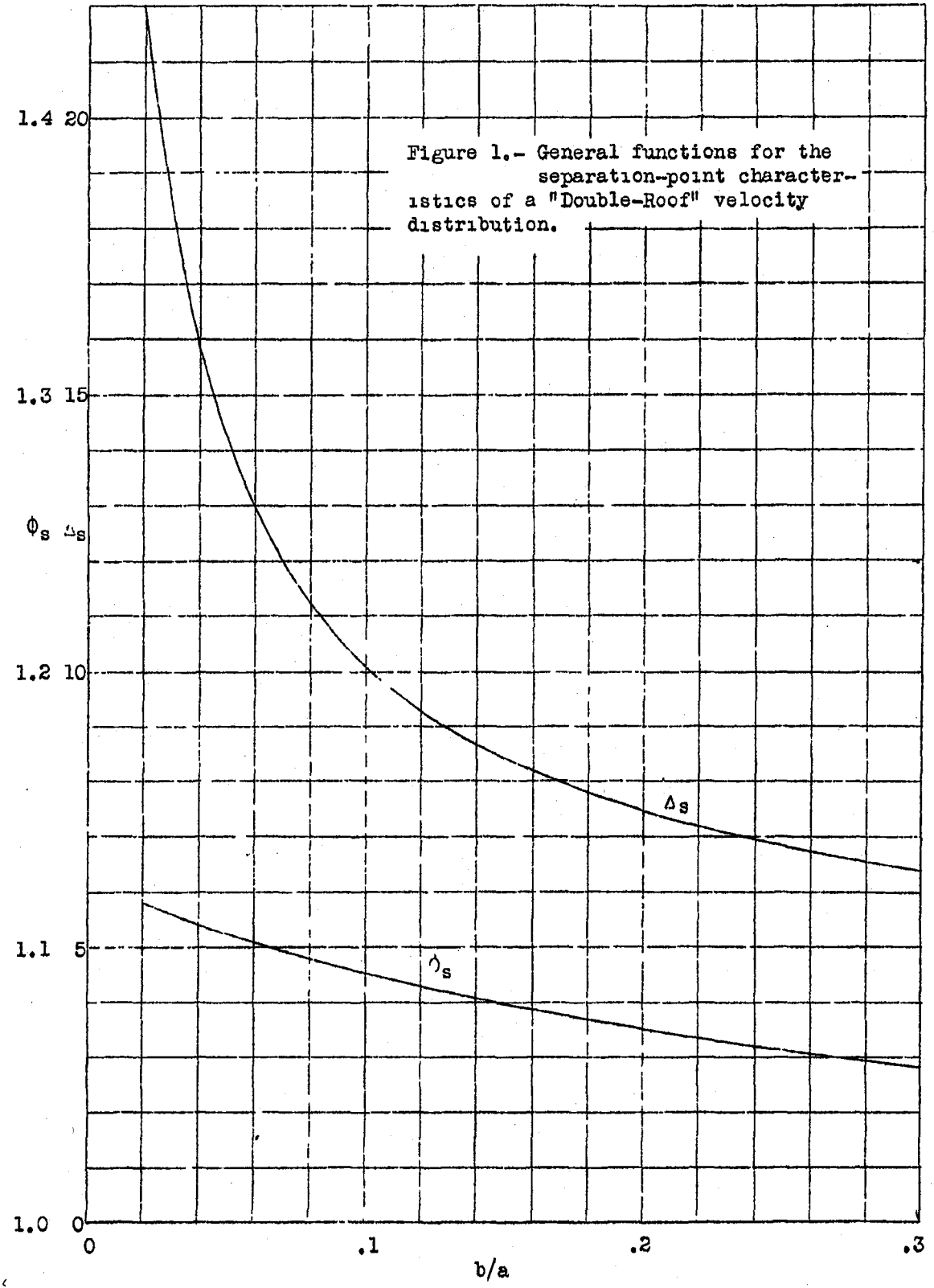

Figure 1.- General functions for the separation-point characteristics of a "Double-Roof" velocity distribution.

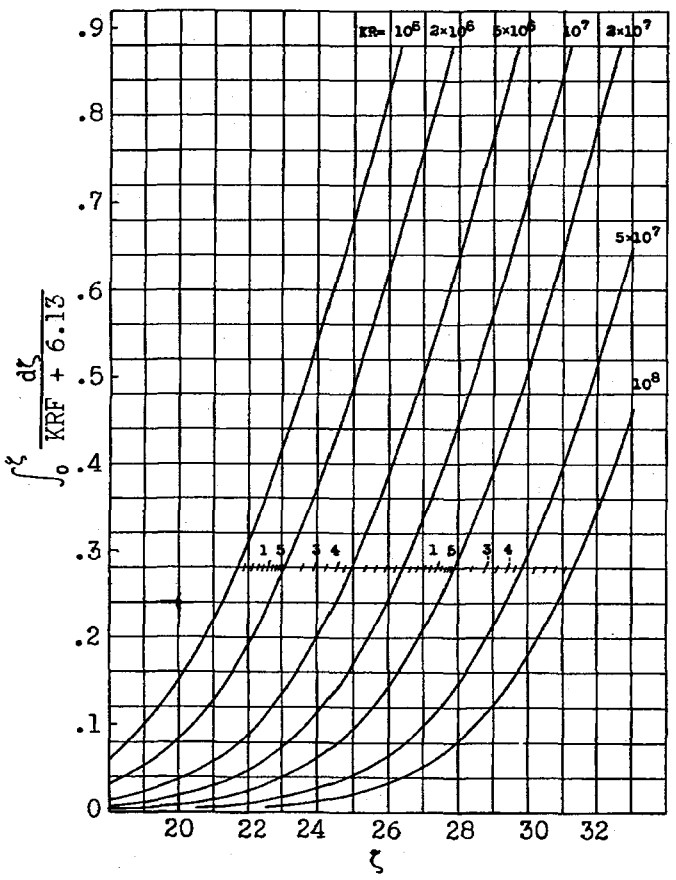

Figure 2.- Graph for evaluating turbulent ζ-factor in regions of decreasing velocity.

(1 block = 10 divisions on 1/50" Engr scale)

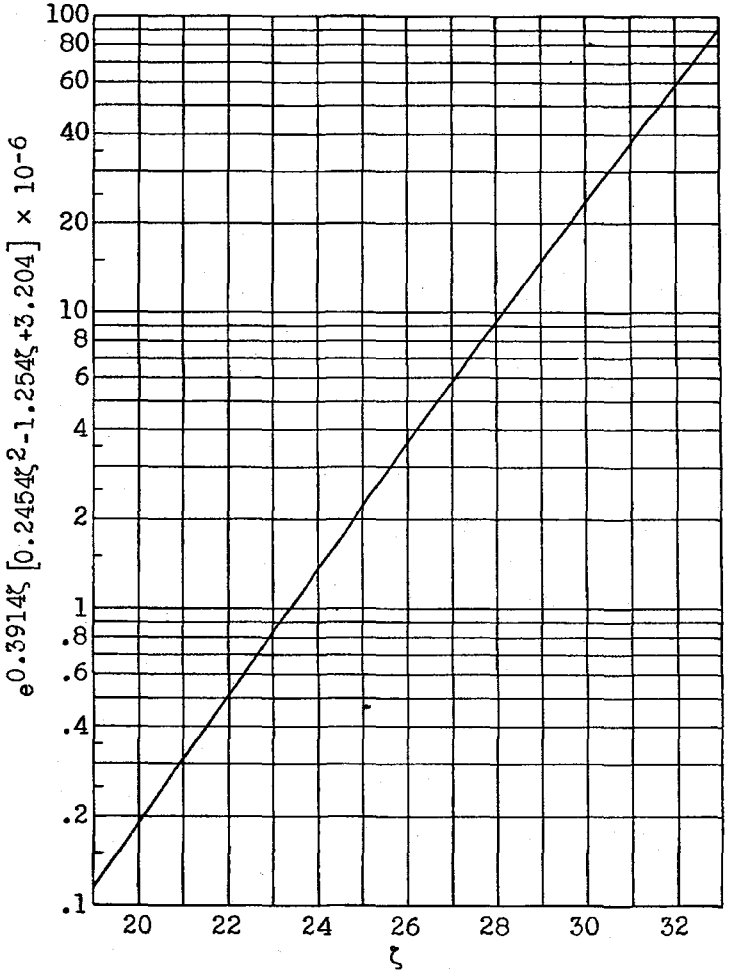

Figure 3.- Graph for evaluating turbulent ζ-factor in regions of constant velocity.

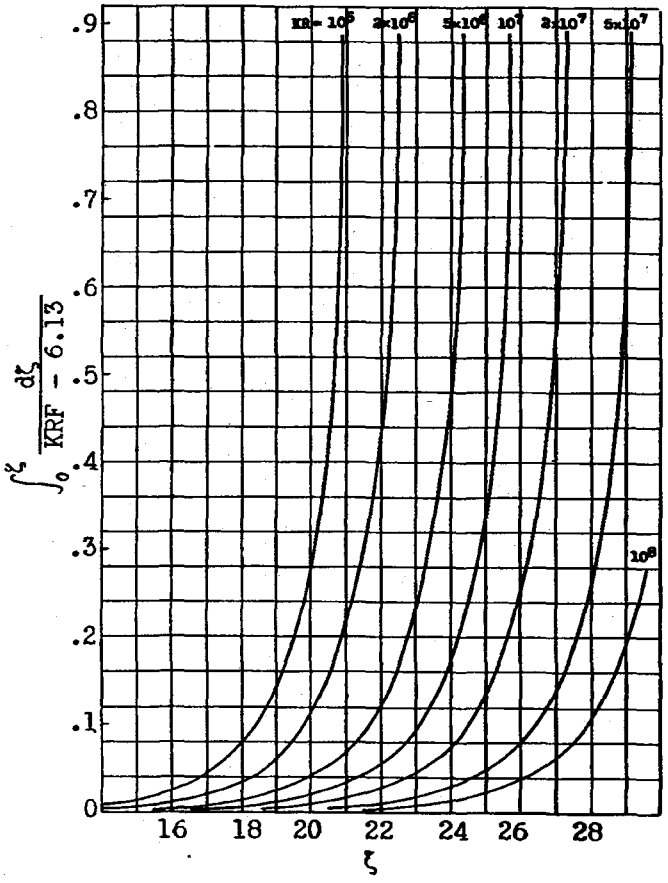

Figure 4.- Graph for evaluating turbulent ζ-factor in regions of increasing velocity.

(1 block = 10/50")

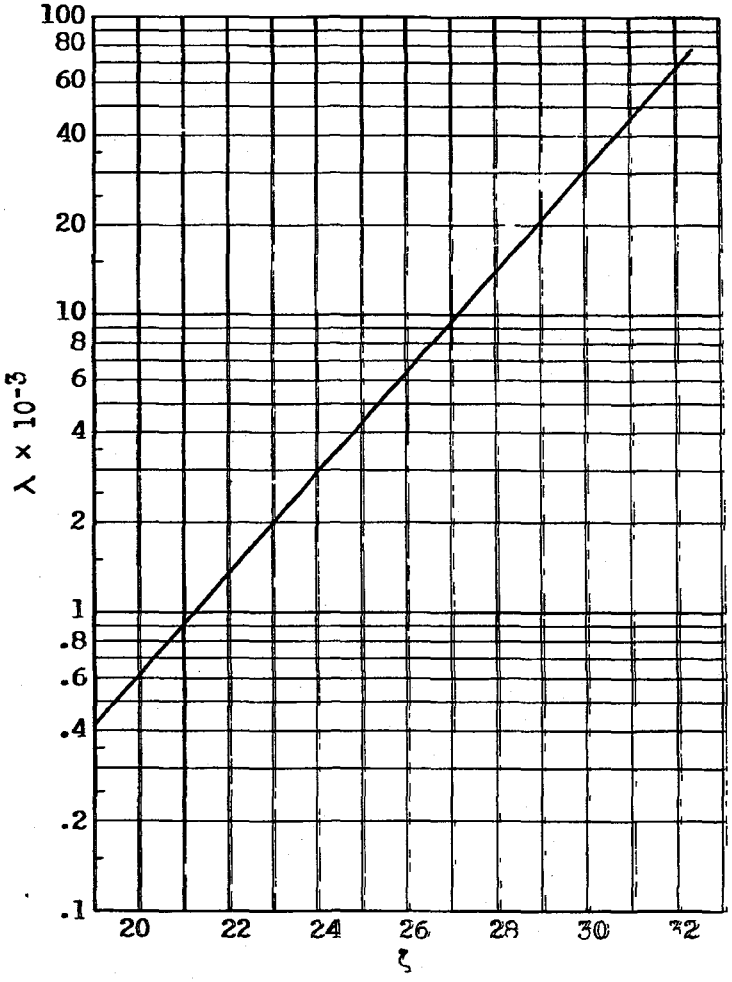

Figure 5.- Variation of λ with turbulent ζ-factor.

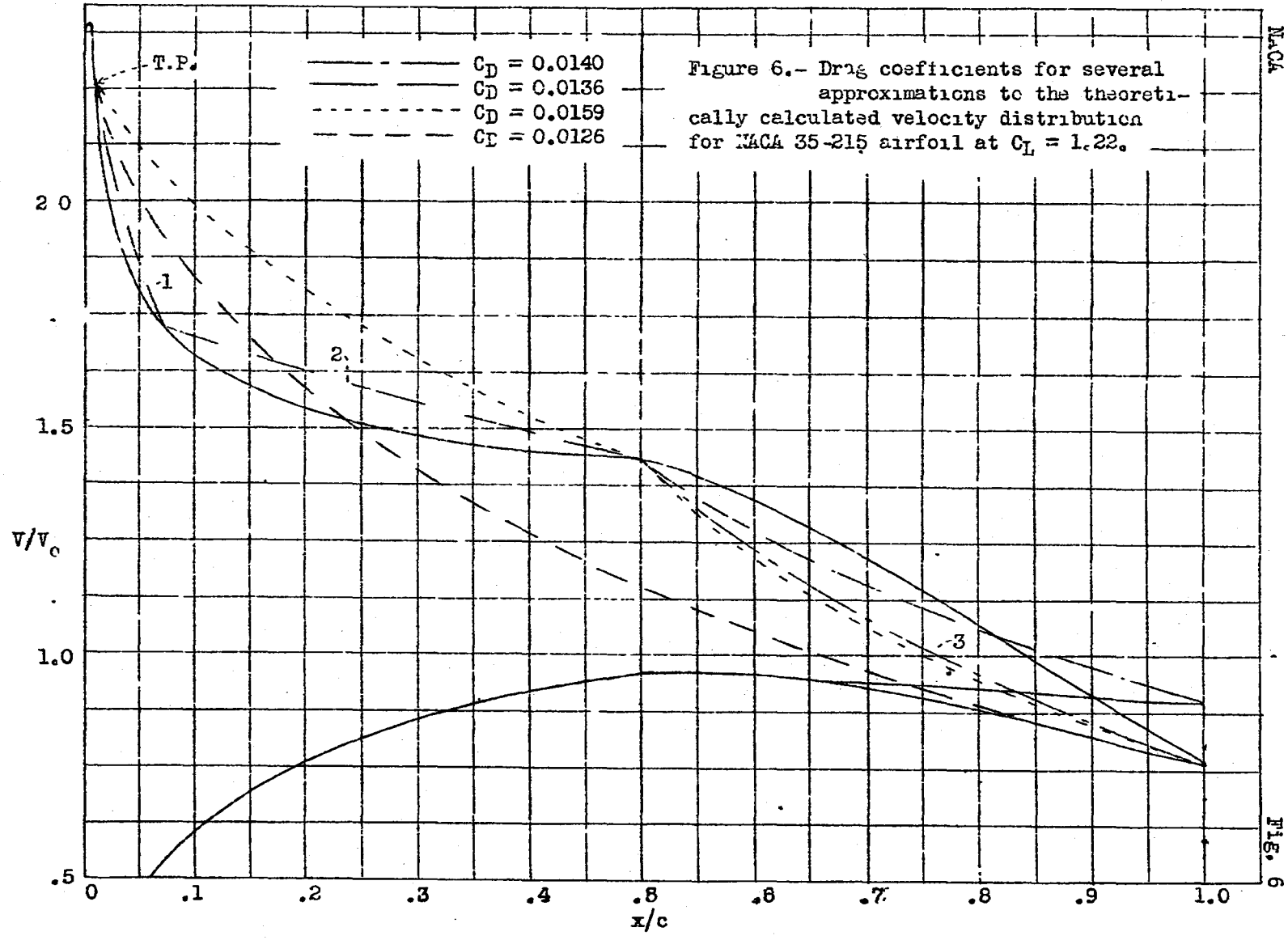

Figure 6.- Drag coefficients for several approximations to the theoretically calculated velocity distribution for NACA 35-215 airfoil at C_L = 1.22.

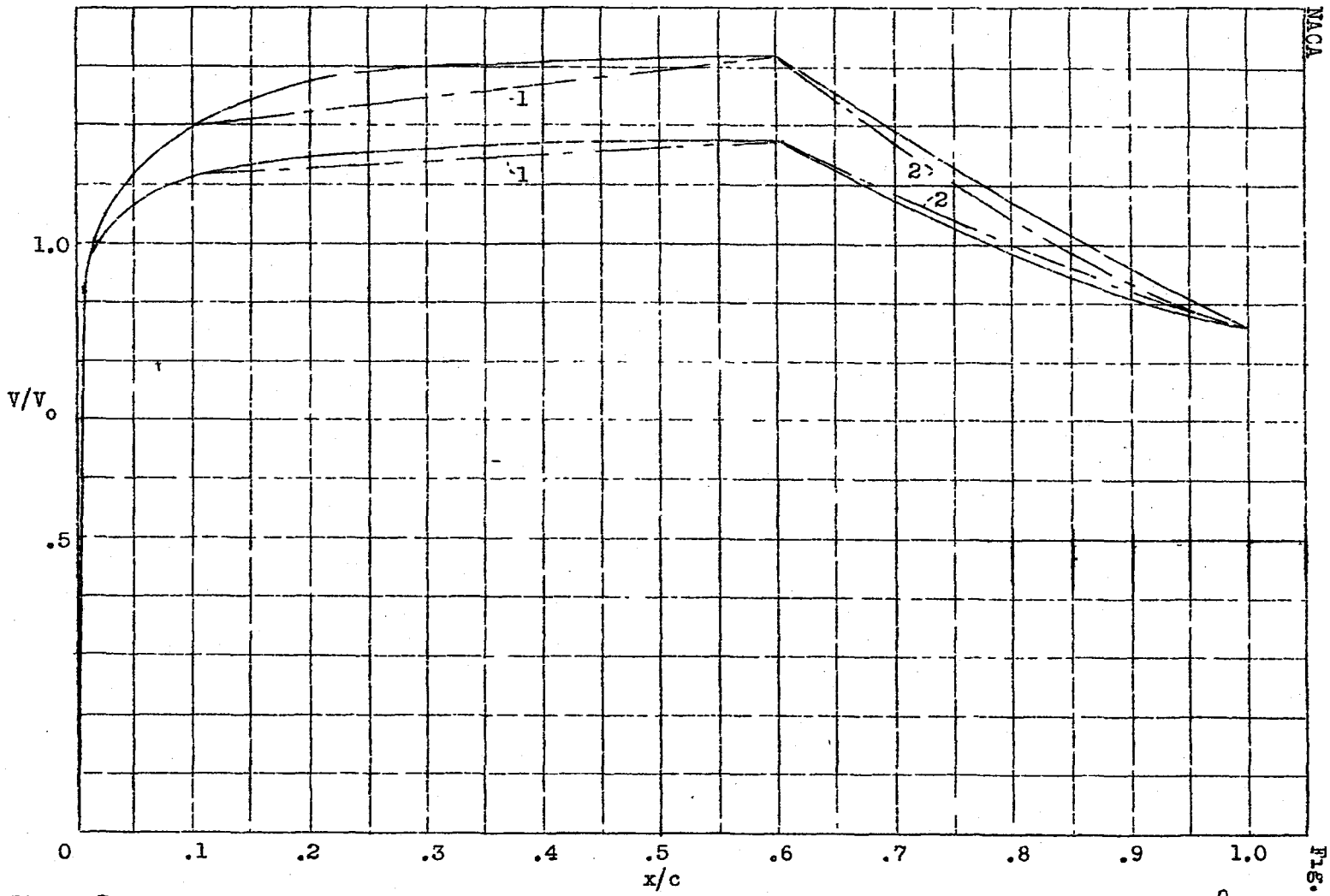

Figure 7.- Approximation to experimental velocity distribution for NACA 66,2-420 airfoil at $\alpha = 0^{\circ}$; transition fixed at x/c = 0.10.

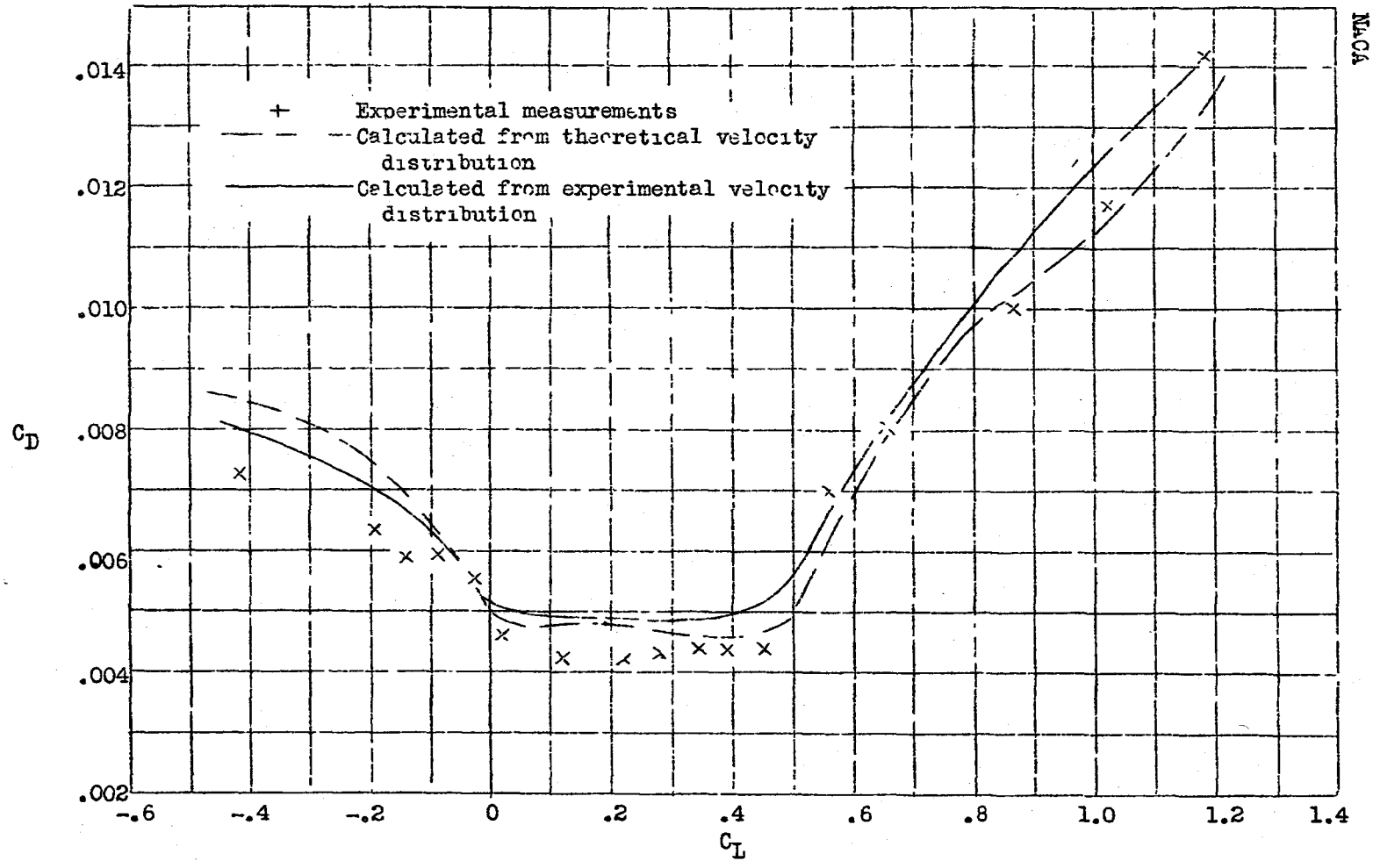

Figure 8.- Comparison of calculated and experimentally measured polars for NACA 35-215 airfoil at $R = 5.75 \times 10^6$.

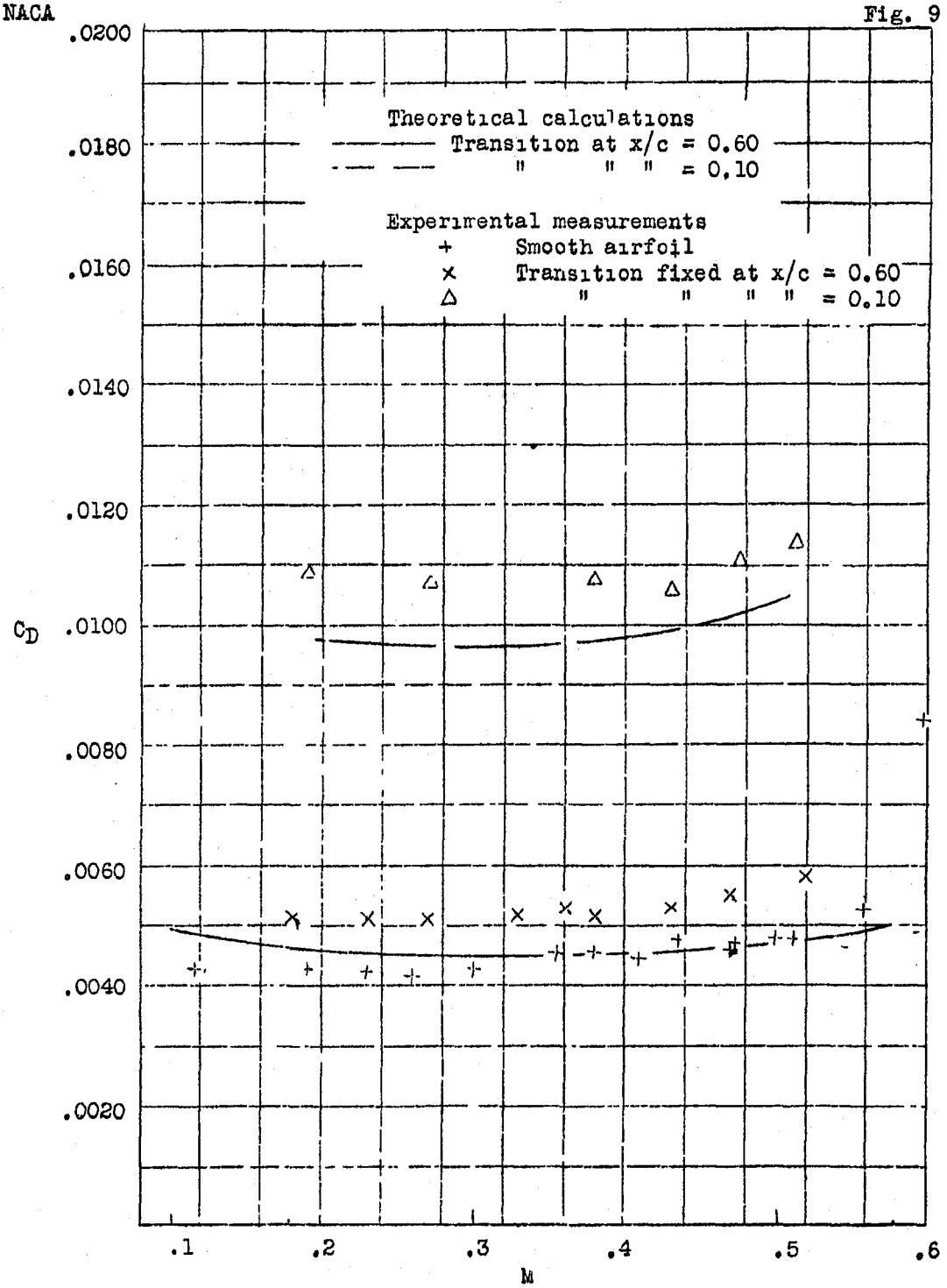

Figure 9.- Comparison of calculated profile drag coefficients with measured values at various Mach numbers for NACA 66,2-420, $\alpha = 0^\circ$.

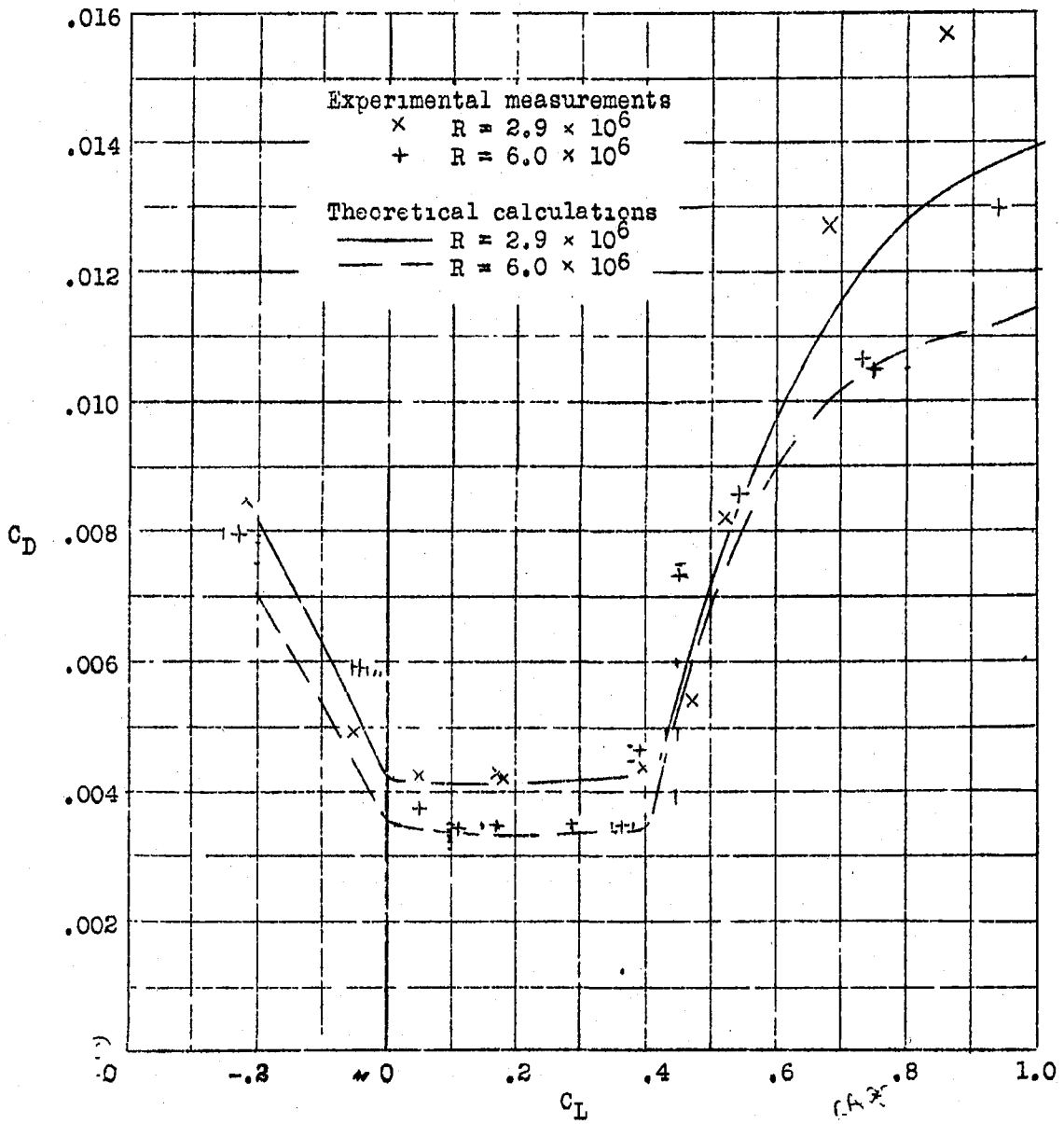

Figure 10.- Comparison of calculated and experimentally measured polars for NACA 67,1-215 airfoil.

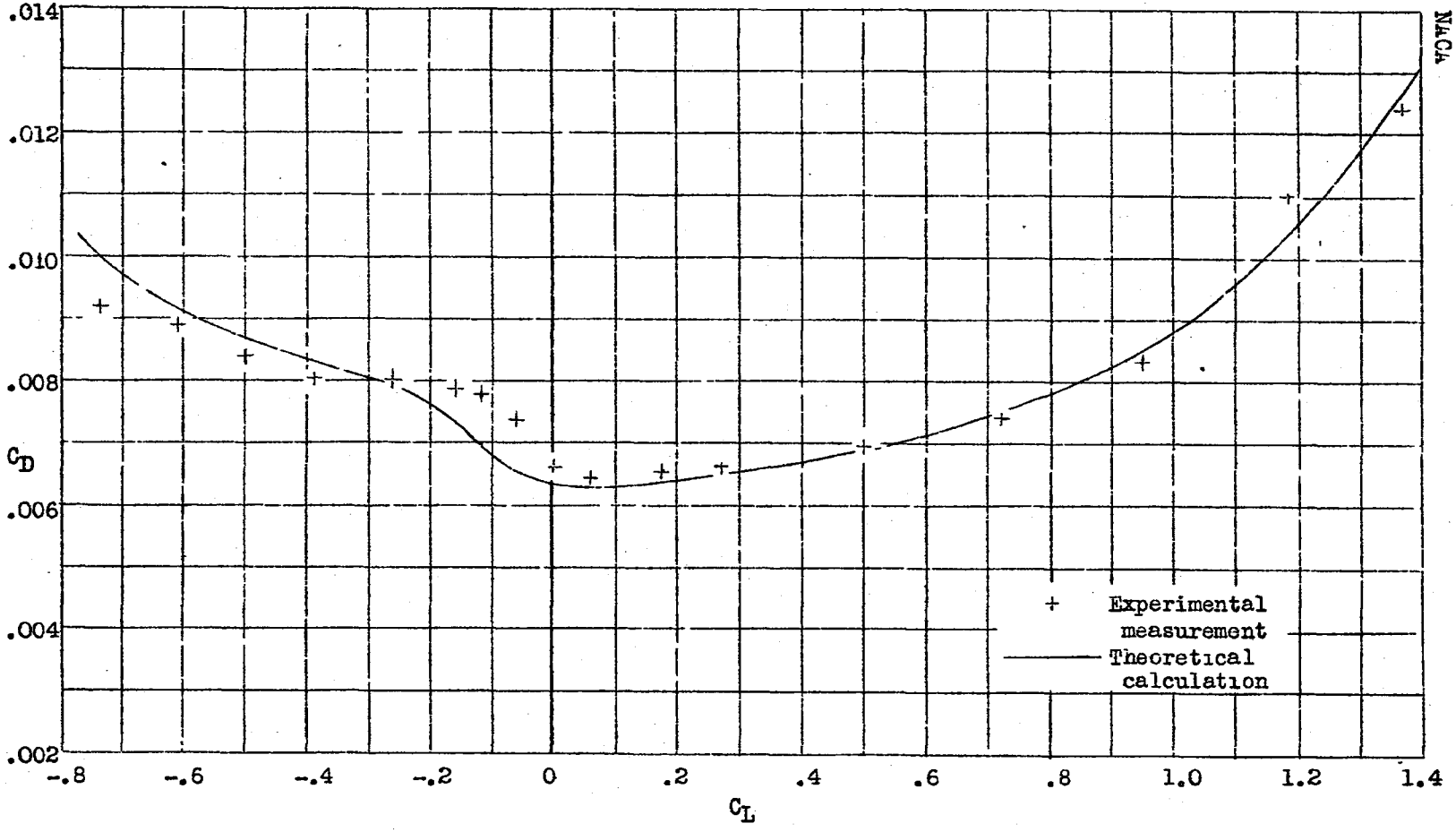

Figure 11.- Comparison of calculated and experimentally measured polars for NACA 23015 airfoil at $R = 5.9 \times 10^6$.

Fig. 11

End of Document